Dielectrically Confined Stable Excitons in Few-Atom-Thick PbS Nanosheets

Tharaka MDS Weeraddana, Shashini M. Premathilaka, Yiteng Tang, Antara Debnath Antu, Adam Roach, Jun Yang, and Liangfeng Sun*

Cite This: *J. Phys. Chem. Lett.* 2022, 13, 7756−7761

Read Online

ACCESS | Metrics & More | Article Recommendations | SI Supporting Information

ABSTRACT: Two-dimensional colloidal PbS nanosheets exhibit more than one order of magnitude larger exciton binding energy than their bulk counterpart, making it possible to generate stable excitons at room temperature. It is experimentally revealed that the binding energy of the exciton increases from 26 to 68 meV as the thickness of the PbS nanosheet decreases from 4.7 to 1.2 nm. The dielectric confinement of the exciton plays a critical role in the binding-energy enhancement. The large binding energy results in a fast thickness-dependent exciton radiative recombination rate, confirmed experimentally.
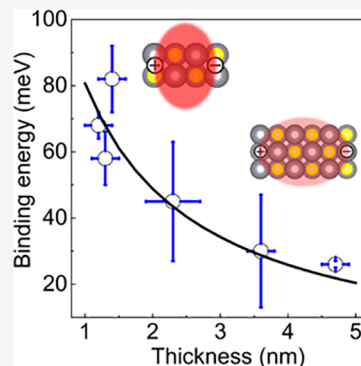
Colloidal semiconductor nanosheets, as one type of emerging two-dimensional nanomaterials, exhibit many unique properties. They include high photoluminescence efficiencies,[1] narrow emission line widths,[1,2] fast emissions,[2] low lasing thresholds,[3] high multiple exciton generation rates,[4] and fast resonance energy transfers.[5] The stability of excitons plays a critical role in these properties. For many infrared materials (e.g., PbS), the exciton binding energy is too small to form stable excitons at room temperature. However, it can be enhanced in a two-dimensional structure—a nanosheet. While theoretical studies have predicted that the binding energy in a PbS nanosheet can reach 80 meV,[6] a direct measurement of the exciton binding energy is still lacking.

In this work, we directly measure the exciton binding energy of nanosheets of different thicknesses. We find that stable excitons can exist at room temperature in PbS nanosheets less than 5 nm thick due to the enhancement of the binding energy. By comparing the theoretical model with the experimental results, we reveal that the dielectric confinement of the exciton enhances its binding energy. The enhanced binding energy leads to a faster radiative decay of the exciton, which is confirmed experimentally.

Colloidal PbS nanosheets have been synthesized using wet-chemistry methods (Supporting Information A).[7−14] The thickness dispersion of the nanosheets is typically large, resulting in inhomogeneous broadening that smears the exciton peak in the optical absorption spectrum. To reduce the inhomogeneous broadening, we modify earlier methods to synthesize more uniform nanosheets (Supporting Information B).[11] We use 1-chlorotetradecane as the cosolvent in the reaction solution. Since it has a long carbon chain, it slows down the growth and the oriented attachment of the nanocrystals. Consequently, nanosheets with small lateral sizes (∼20 × 20 nm) and uniform thickness are synthesized (Figure 1a). The X-ray diffraction (XRD) shows the nanosheet has a rock-salt crystal structure (galena) with a (100) basal plane (Supporting Information C). We determine the thickness of the nanoplatelets using transmission electron microscopy (TEM) and XRD. Both methods show the same
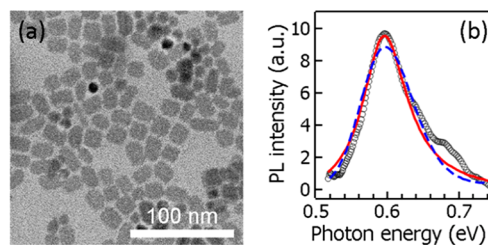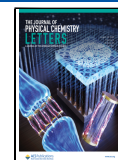

Figure 1. (a) The TEM image of the nanosheets with an average lateral size of 20 × 20 nm. (b) The photoluminescence (PL) peak (circles) with its Gaussian (dashed line) and Lorentzian (solid line) fitting curves.

average thickness of 4.7 nm, which is about 16 monolayers (MLs) of atoms. The thickness dispersion (one standard deviation) is 0.2 nm, which is ∼4% of the average thickness.

Such a small thickness dispersion results in a sharp emission peak from the nanosheets. Since the thickness determines the energy gap of the nanosheets[9] and therefore the energy of the emitted photons, the dispersion of the thickness determines the inhomogeneous broadening of the photoluminescence peak. The uniform nanosheets result in a narrow emission line width with its full-width-at-half-maximum of ∼70 meV (Figure 1b), which is only half of the line width from the typical nanosheets.[9] The line shape of the emission is more Lorentzian-like than Gaussian-like (Figure 1b),[15] which could be the consequence of a narrow and discrete thickness distribution.

More importantly, the uniformity of the nanosheets distinguishes the exciton peak from the continuum in the optical absorption spectrum. At room temperature, the bulk PbS shows no exciton peak[16] due to the small oscillator strength of the exciton. The exciton peak near the band edge of the nanosheet (Figure 2a) indicates enhanced oscillator strength of the exciton when it is confined in this two-dimensional structure. However, this feature could be obscured if the thickness dispersion of the nanosheets is large[6] as shown in the earlier literature.[4,7,9]

The optical absorption near the band edge includes the excitonic and continuum contributions. We fit the absorption spectrum $\alpha(E_p)$ (where E_p is the photon energy) using a semiempirical equation[17]

$$\alpha(E_p) = \frac{\alpha_c \sqrt{E_p - 0.41}}{1 + \exp\left[\frac{E_c - E_p}{\Gamma_c}\right]} + \alpha_e \exp\left[-\frac{(E_p - E_e)^2}{2(\Gamma_e)^2}\right] \tag{1}$$

It is the sum of a broadened two-dimensional continuum and an exciton peak. The continuum is modeled as a broadened step function where E_c is the energy of the continuum edge, and Γ_c is the broadening. Since the nanosheets are not strictly two-dimensional,[16] the term $\sqrt{E_p - 0.41}$ (where 0.41 eV is the bandgap energy of the bulk PbS at room temperature) is used to account for the increase of the density of states by the energy.[18] The exciton peak is modeled by a Gaussian function, where E_e is the energy corresponding to the exciton peak, and Γ_e represents the broadening. Though the 4.7 nm thick nanosheets are uniform enough to show a Lorentzian line shape, nanosheets of other thicknesses have a Gaussian line shape. We use a Gaussian function for all the exciton peaks to keep the model consistent.

We fit the optical absorption spectra of a series of nanosheets of different thicknesses using eq 1. The fitting curves for 4.7 nm (16 MLs), 3.6 nm (12 MLs), 2.3 nm (8 MLs), and 1.3 nm (4 MLs) thick nanosheets are shown in Figure 2, while additional ones are shown in the Supporting Information D. The fitting curve $\alpha(E_p)$ matches with the absorption spectrum of the 4.7 nm thick nanosheets (Figure 2a). The energy difference between the continuum edge E_c (0.610 eV) and the exciton peak E_e (0.584 eV) gives the binding energy of the exciton (26 meV) (Table 1).[19] It is 10 times larger than the exciton binding energy in a PbS bulk (2.6 meV, see Supporting Information E).
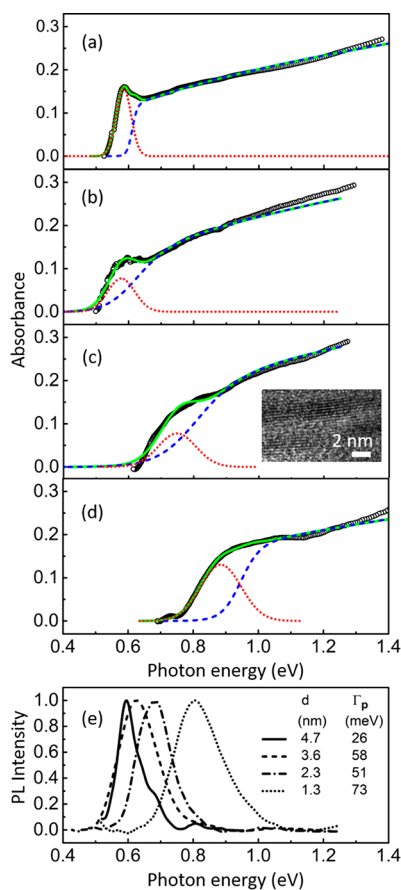
Figure 2. Optical absorption spectra (circles) of the nanosheets dispersed in tetrachloroethene, with thicknesses of (a) 4.7 nm, (b) 3.6 nm, (c) 2.3 nm, and (d) 1.3 nm. Each solid line is an empirical fit that is the sum of a Gaussian exciton peak (dashed line) and a broadened continuum (dotted line). Inset of (c): the high-resolution TEM image of the edges of the nanosheets showing eight layers of atoms with an interlayer spacing of 0.3 nm. (e) The photoluminescence (PL) spectra of the nanosheets. Γ_p is the broadening (standard deviation of the Gaussian function fitting the PL peak) of the emission peak (Supporting Information F).

Table 1. Nanosheet Thicknesses (d), Binding Energies (E_b), Exciton Peak Energies (E_e), Broadenings (Γ_e), Photoluminescence Peak Energies E_p, and Broadenings Γ_p[a]

d (nm)	E_b (meV)	E_e (meV)	Γ_e (meV)	E_p (meV)	Γ_p (meV)
4.7 ± 0.2	26	584	23	601	26
3.6 ± 0.2	30	578	42	631	58
2.3 ± 0.4	45	749	58	680	51
1.4 ± 0.2	82	1102	77	1039	73
1.3 ± 0.2	58	885	63	816	73
1.2 ± 0.2	68	865	77	843	66

[a]The complete fitting results including the fitting errors are shown in Supporting Information F.

As the nanosheets get thinner, the optical absorption and emission spectra shift to higher energies (from 0.6 to 1.1 eV) due to the quantum confinement in the thickness direction (Figure 2). The crystal structure[13] and the lateral size[20] (if small enough) could affect the energy gap. These, however, do not apply in our case, since the nanosheets have the same cubic crystal structure, and their lateral sizes are large. The binding energy also increases as the thickness decreases (Table 1). For each sample, the width of the exciton emission peak

(photoluminescence) is close to the width of the absorption peak (Table 1), indicating a common broadening source. The thin nanosheets (1.2, 1.3, 1.4, and 2.3 nm) experience Stokes shifts, but the thick ones (3.6 and 4.7 nm) experience anti-Stokes shifts. It is likely the result of the interplay among the thickness dispersion, thickness-dependent photoluminescence efficiency,[21] and defect states[22] (discussed in Supporting Information G).

Both 4.7 and 3.6 nm thick nanosheets show clear exciton peaks in their optical absorption spectra. The exciton peaks of the thinner nanosheets are less clear, likely due to the thickness dispersion. However, the data fitting for each absorption spectrum converges to the same values even if we change the initial values of the fitting parameters in a broad range, suggesting the robustness of the fitted parameters.

The enhancement of the binding energy is likely caused by both dimensional and dielectric confinements of the exciton in the thin nanosheet. As the thickness of the nanosheet goes below the Bohr radius of the exciton, the electron and the hole are squeezed in the thickness direction but are free to move in the lateral direction, making it pancake-like. The strong confinement in the thickness direction results in quantized energy levels h^2/md^2 (h: Planck constant; m: mass of the charge carrier) that are inversely proportional to the square of the thickness (d). The consequence is the blueshift of the absorption and emission spectra as the nanosheets get thinner (Figure 2).

On the other hand, the dimensional confinement of the exciton increases the spatial overlap between the electron and the hole. Theoretically, the binding energy of a two-dimensional exciton is 4 times larger than that of a three-dimensional exciton.[23,24] Moreover, the small dielectric constant of the surrounding medium enhances the electron–hole Coulomb interaction, since the electric field is less screened there (Figure 3, inset). As the thickness decreases, the
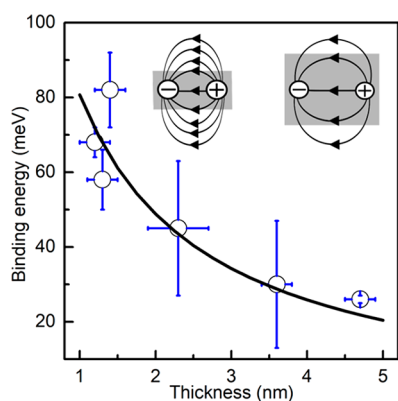
Figure 3. Dependence of the binding energy on the thickness of the nanosheet (circles) and the fitting curve (solid line) based on Keldysh's theory. Inset: the electric field indicated by the field lines between the electron (−) and the hole (+) is stronger in a thin nanosheet than in a thick nanosheet.

exciton in the nanosheet "sees" more of the small-dielectric-constant medium than the large-dielectric-constant core. Therefore, the Coulomb interaction between the electron and the hole is enhanced and so is the binding energy. In semiconductor quantum wells on a substrate, only the excitons near the surface where an abrupt change of the dielectric constant occurs have their binding energies enhanced.[25] In the

free-standing colloidal nanosheet, all the excitons are expected to have enhanced binding energies.

The enhancement of the electron–hole Coulomb interaction in a thin semiconductor film (or a quantum well) was first described by Keldysh's theory.[26] The relative motion of the charges of an exciton is considered two-dimensional. The potential energy comes from the Coulomb interactions among the charges and image charges.[26,27] When the thickness of the film d satisfies the condition $a_0 \gg d \gg \left(\frac{\varepsilon_2}{2\varepsilon_1}\right)^2 a_0$ (Supporting Information H), the energy of the ground state of the exciton is obtained by solving the two-dimensional Schrödinger equation[26,28]

$$E_1 = -\frac{e^2}{4\pi\varepsilon_0\varepsilon_1 d}\left[\ln\left(\frac{d}{a_0}\left(\frac{2\varepsilon_1}{\varepsilon_2}\right)^2\right) - 2.298\right] \tag{2}$$

where a_0 is the Bohr radius of the exciton in bulk PbS ($a_0 = \frac{4\pi\varepsilon_0\varepsilon_1\hbar^2}{e^2}$), and e and $\hbar$ are the charge of the electron and the reduced Planck constant, respectively. μ, ε_0, ε_1, and ε_2 are the reduced effective mass of the exciton, the vacuum permittivity, the dielectric constant of the semiconductor, and the dielectric constant of the surrounding medium, respectively. The coupling of the excited states to light is reduced compared to the ground state so that their spectral weight decreases with the increasing quantum number,[19] and they quickly blend into a continuum.[6] Therefore, we only consider the binding energy (E_b) of the ground state of the exciton where $E_b = -E_1$.

To obtain the best fit of the experimental data with the theoretical model described by eq 2, we have to consider the change of the physical parameters (e.g., effective mass and dielectric constant) as the size of the material is reduced to the nanoscale. For two-dimensional quantum wells[29] or nanosheets,[6,30] the effective mass of the electron or the hole increases as the thickness decreases to a few nanometers. A modified Kane formula shows the effective mass depends on the confinement energy.[29,31] The dependence can be parametrized[29] by $m_{eff} = m_0^*/(1 - (\beta/(cd + f)))$, where d is the thickness and m_0^* is the effective mass of the electron in the bulk (∼0.12 m_0, m_0 is the free electron mass).[32] Since the difference between the effective masses of the hole (m_h) and the electron (m_e) is little,[32] we use m_{eff} to represent both of them: $m_h = m_e = m_{eff}$. The other parameters (β, c, and f) are fitting parameters.

Since the Coulomb interaction between the electron and the hole depends on the electron–hole (e–h) distance r (the average separation distance between the electron and the hole),[27] the dielectric constant of the nanosheet is then a function of r

$$\varepsilon_1(r) = \frac{1}{\frac{1}{\varepsilon_1^\infty} - \left(\frac{1}{\varepsilon_1^\infty} - \frac{1}{\varepsilon_1^0}\right)\left[1 - \frac{1}{2}(e^{-q_e r} + e^{-q_h r})\right]} \tag{3}$$

with $q_e = \left(\frac{2m_e\omega}{\hbar}\right)^{0.5}$ and $q_h = \left(\frac{2m_h\omega}{\hbar}\right)^{0.5}$ where ω is the longitudinal optical (LO) phonon frequency. The LO-phonon energy ($\hbar\omega$) in PbS is 26.6 meV, from which q_e and q_h can be obtained. We derive the phonon energy from the Raman spectrum of PbS nanocrystals that are 3 nm large (Supporting Information I), which is close to the thickness of our

nanosheets. We assume the phonon energy is a constant for all the nanosheets. It could change when the nanosheet is extremely thin, as reported for perovskite nanoplatelets.[33,34]

The calculation based on the $k \cdot p$ model shows that the e–h distance r has a linear dependence on the nanosheet thickness d.[6] Therefore, we use $ad + b$ (where a and b are constants to be fit) to replace r in eq 3, making $\varepsilon_1(r)$ a function of the nanosheet thickness d. The room temperature (300 K) static dielectric constant ε_1^0 and optical dielectric constant ε_1^∞ are 172 and 17, respectively.[35] We set ε_2 of the oleic acid molecules capping the PbS nanosheet to be 1.9.

The dependence of the binding energy on the thickness is well fit (Figure 3) by using eq 2. Meanwhile, we obtain the dependences of the charger-carrier effective mass and the e–h distance on the thickness (Figure 4). Based on the fitting
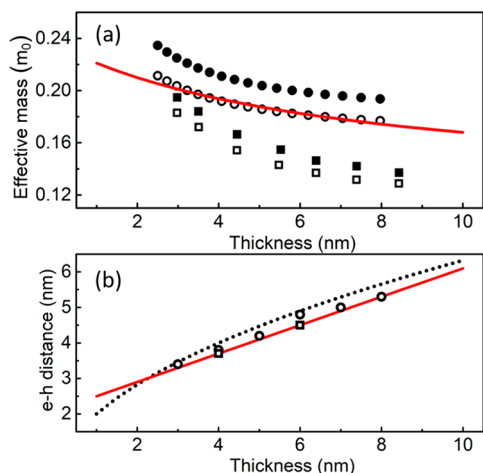

Figure 4. (a) The dependence of the effective mass of the charge carrier on the thickness of the nanosheet (solid line). The effective masses obtained by other methods: $k \cdot p$ model computation[6] (electron, solid circles; hole, open circles) and OPTPS[30] (electron, solid squares; hole, open squares) are shown for comparison. (b) The dependences of the e−h distance on the thickness of the nanosheets based on our results (solid line), Lauth's experiments[30] (open squares), Yang's computation[6] (open circles), and Keldysh's theory[26] (dotted line).

curve, the binding energy decreases from 80 to 20 meV as the thickness increases from 1 to 5 nm. In the thickness range from 3 to 5 nm, the binding energy is between 34 and 20 meV, smaller than that predicted by the $k \cdot p$ model: 70 to 45 meV.[6] The $k \cdot p$ model could overestimate the binding energy, which was also noticed in Lauth's work for thicker nanosheets.[30] The charge-carrier effective mass increases as the thickness of the nanosheet decreases (Figure 4a). It matches up with the computational results based on the $k \cdot p$ model,[6] but the effective mass is slightly larger than that derived from optical pump-terahertz probe spectroscopy (OPTPS).[30]

The linear dependence of the e–h distance on the thickness (Figure 4b) is consistent with the calculated results based on the $k \cdot p$ model.[6] It shows the e–h distances for 4 and 6 nm thick nanosheets are 3.7 and 4.5 nm, respectively, which are the same as the Bohr radii derived from OPTPS.[30] The e–h distance predicted by Keldysh's theory $((a_0 d)^{1/2}/2)$ is slightly off.[26] It is likely due to the fixed effective mass and dielectric constant used there. The e–h distance in the nanosheet is smaller than that in bulk PbS. For a hydrogenic exciton in a bulk PbS, the e–h distance for the lowest-energy s-like exciton

is 24 nm ($1.5a_0$, $a_0 \approx 16$ nm calculated with an optical dielectric constant). If the exciton in a PbS nanosheet is considered two-dimensional in a homogeneous medium, its average e–h distance will reduce to $a_0/2$.[24,36] It is still larger than what we obtained from the experiments (Figure 4b). The further reduction of the e–h distance is likely due to the dielectric confinement. The e–h distance in the nanosheet (<4 nm) is much smaller than the smallest lateral size (∼20 nm) of the nanosheets under our study. Therefore, the confinement in the lateral dimension is negligible, and the exciton motion can be considered two-dimensional.

The reduced e−h distance in a two-dimensional exciton leads to enhanced oscillator strength (Supporting Information J) and fast radiative recombination of the exciton. The latter can be measured experimentally. We measured photoluminescence decay rates (R_{PL}) and absolute quantum yields (η) of three batches of thin nanosheets with thicknesses of 1.4, 1.6, and 2.2 nm, respectively. As the nanosheet thickness decreases, the photoluminescence decay rate decreases, while the quantum yield increases (Supporting Information K). The surface defects are the main cause of the nonradiative decay, since surface passivation of the as-synthesized nanosheets can dramatically improve the quantum yield.[14] Since the thickness dispersion of each set of nanosheets is small, we can treat the radiative recombination rate (R_{rad}) in each sample as a constant. Assuming the nonradiative decay rate is R_{nrad}, we have $\eta = R_{rad}/(R_{rad} + R_{nrad})$ and $R_{rad} = \eta R_{PL}$.[37,38] From the time-resolved photoluminescence data and the quantum yield, we obtain the radiative recombination rate. It increases as the thickness (d) decreases (Figure 5 inset).
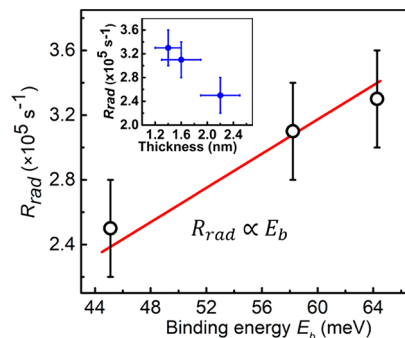
Figure 5. Dependence (solid line) of the measured exciton radiative recombination rate R_{rad} (circles) on the binding energy. Inset: thickness-dependent radiative recombination rate.

Using the relationship between the binding energy E_b and the thickness d described in eq 2, we find R_{rad} has a $1/d$ dependence on the thickness (Figure 5). Feldmann and co-workers discovered the same dependence for the excitons in GaAs/AlGaAs quantum wells at a low temperature (5 K).[39] Their theoretical analysis shows that the free exciton radiative recombination rate (R_{rad}) is proportional to the oscillator strength, and the latter is proportional to the binding energy of a quasi-two-dimensional exciton. Therefore, R_{rad} is proportional to the binding energy, which applies to our nanosheets too. In zero-dimensional PbS quantum dots, the radiative recombination rate, which is the inverse of the exciton radiative lifetime, increases as the size of the quantum dot decreases,[40] showing a similar trend as in PbS nanosheets.

In conclusion, we have created uniform few-atom-thick colloidal PbS nanosheets where stable excitons exist at room

temperature. The contrast of the dielectric constants between the PbS core and the organic surface ligands creates dielectric confinement on the excitons in the PbS core, dramatically increasing the exciton binding energy. The e−h distance in a nanosheet is much smaller than that in a bulk PbS. The shrink of the e−h distance increases the exciton oscillator strength and the radiative recombination rate. They are advantageous for efficient and fast light-emitting, optical gain, and lasing. The moderate exciton binding energy is also suitable for photovoltaic applications, since the exciton dissociation can occur with a proper energy-level alignment in a device.

■ ASSOCIATED CONTENT

ⓢ Supporting Information

The Supporting Information is available free of charge at https://pubs.acs.org/doi/10.1021/acs.jpclett.2c02254.

> Typical synthesis of PbS nanosheets, synthesis of uniform nanosheets, thickness of the nanosheets, additional absorption spectra and fitting curves, the Rydberg constant of bulk PbS, fitting results, anti-Stokes shift, Keldysh's thickness condition, LO-phonon energy, oscillator strength, and photoluminescence decay rate and quantum yield (PDF)

■ AUTHOR INFORMATION

Corresponding Author

Liangfeng Sun − *Center for Photochemical Sciences, Bowling Green State University, Bowling Green, Ohio 43403, United States; Department of Physics and Astronomy, Bowling Green State University, Bowling Green, Ohio 43403, United States;* ⓘ orcid.org/0000-0003-0527-1777; Email: lsun@bgsu.edu

Authors

Tharaka MDS Weeraddana − *Department of Physics and Astronomy, Bowling Green State University, Bowling Green, Ohio 43403, United States;* ⓘ orcid.org/0000-0002-8042-9629

Shashini M. Premathilaka − *Center for Photochemical Sciences, Bowling Green State University, Bowling Green, Ohio 43403, United States; Department of Physics and Astronomy, Bowling Green State University, Bowling Green, Ohio 43403, United States*

Yiteng Tang − *Center for Photochemical Sciences, Bowling Green State University, Bowling Green, Ohio 43403, United States; Department of Physics and Astronomy, Bowling Green State University, Bowling Green, Ohio 43403, United States;* ⓘ orcid.org/0000-0002-7533-756X

Antara Debnath Antu − *Department of Physics and Astronomy, Bowling Green State University, Bowling Green, Ohio 43403, United States*

Adam Roach − *Center for Photochemical Sciences, Bowling Green State University, Bowling Green, Ohio 43403, United States; Department of Physics and Astronomy, Bowling Green State University, Bowling Green, Ohio 43403, United States*

Jun Yang − *Corning Research & Development Corporation, Painted Post, New York 14870, United States*

Complete contact information is available at:
https://pubs.acs.org/10.1021/acs.jpclett.2c02254

Author Contributions

The manuscript was written through contributions of all authors. All authors have given approval to the final version of the manuscript.

Notes

The authors declare no competing financial interest.

■ ACKNOWLEDGMENTS

■ REFERENCES

(1) Liu, Y.; Wayman, V. L.; Gibbons, P. C.; Loomis, R. A.; Buhro, W. E. Origin of High Photoluminescence Efficiencies in CdSe Quantum Belts. *Nano Lett.* **2010**, *10*, 352−357.

(2) Ithurria, S.; Tessier, M. D.; Mahler, B.; Lobo, R. P. S. M.; Dubertret, B.; Efros, A. L. Colloidal Nanoplatelets with Two-Dimensional Electronic Structure. *Nat. Mater.* **2011**, *10*, 936−941.

(3) She, C.; Fedin, I.; Dolzhnikov, D. S.; Demortière, A.; Schaller, R. D.; Pelton, M.; Talapin, D. V. Low-Threshold Stimulated Emission using Colloidal Quantum Wells. *Nano Lett.* **2014**, *14*, 2772−2777.

(4) Aerts, M.; Bielewicz, T.; Klinke, C.; Grozema, F. C.; Houtepen, A. J.; Schins, J. M.; Siebbeles, L. D. A. Highly Efficient Carrier Multiplication in PbS Nanosheets. *Nat. Commun.* **2014**, *5*, 3789.

(5) Rowland, C. E.; Fedin, I.; Zhang, H.; Gray, S. K.; Govorov, A. O.; Talapin, D. V.; Schaller, R. D. Picosecond Energy Transfer and Multiexciton Transfer Outpaces Auger Recombination in binary CdSe Nanoplatelet Solids. *Nat. Mater.* **2015**, *14*, 484.

(6) Yang, J.; Wise, F. W. Electronic States of Lead-Salt Nanosheets. *J. Phys. Chem. C* **2015**, *119*, 26809−26816.

(7) Schliehe, C.; Juarez, B. H.; Pelletier, M.; Jander, S.; Greshnykh, D.; Nagel, M.; Meyer, A.; Foerster, S.; Kornowski, A.; Klinke, C.; et al. Ultrathin PbS Sheets by Two-Dimensional Oriented Attachment. *Science* **2010**, *329*, 550−553.

(8) Dogan, S.; Bielewicz, T.; Cai, Y.; Klinke, C. Field-effect Transistors made of Individual Colloidal PbS Nanosheets. *Appl. Phys. Lett.* **2012**, *101*, 073102.

(9) Bhandari, G. B.; Subedi, K.; He, Y.; Jiang, Z.; Leopold, M.; Reilly, N.; Lu, H. P.; Zayak, A. T.; Sun, L. Thickness-Controlled Synthesis of Colloidal PbS Nanosheets and their Thickness-Dependent Energy Gaps. *Chem. Mater.* **2014**, *26*, 5433−5436.

(10) Bielewicz, T.; Dogan, S.; Klinke, C. Tailoring the Height of Ultrathin PbS Nanosheets and their Application as Field-Effect Transistors. *Small* **2015**, *11*, 826−833.

(11) Premathilaka, S. M.; Jiang, Z.; Antu, A.; Leffler, J.; Hu, J.; Roy, A.; Sun, L. A Robust Method for the Synthesis of Colloidal PbS Nanosheets. *Phys. Status Solidi RRL* **2016**, *10*, 838−842.

(12) Zhang, H.; Savitzky, B. H.; Yang, J.; Newman, J. T.; Perez, K. A.; Hyun, B.; Kourkoutis, L. F.; Hanrath, T.; Wise, F. W. Colloidal Synthesis of PbS and PbS/CdS Nanosheets using Acetate-Free Precursors. *Chem. Mater.* **2016**, *28*, 127−134.

(13) Khan, A. H.; Brescia, R.; Polovitsyn, A.; Angeloni, I.; Martín-García, B.; Moreels, I. Near-Infrared Emitting Colloidal PbS Nanoplatelets: Lateral Size Control and Optical Spectroscopy. *Chem. Mater.* **2017**, *29*, 2883−2889.

(14) Antu, A. D.; Jiang, Z.; Premathilka, S. M.; Tang, Y.; Hu, J.; Roy, A.; Sun, L. Bright Colloidal PbS Nanoribbons. *Chem. Mater.* **2018**, *30*, 3697−3703.

(15) Ithurria, S.; Bousquet, G.; Dubertret, B. Continuous Transition from 3D to 1D Confinement Observed during the Formation of CdSe Nanoplatelets. *J. Am. Chem. Soc.* **2011**, *133*, 3070−3077.

(16) Scanlon, W. W. Intrinsic Optical Absorption and the Radiative Recombination Lifetime in PbS. *Phys. Rev.* **1958**, *109*, 47−50.

(17) Chemla, D. S.; Miller, D. A. B.; Smith, P. W.; Gossard, A. C.; Wiegmann, W. Room Temperature Excitonic Nonlinear Absorption and Refraction in GaAs/AlGaAs Multiple Quantum Well Structures. *IEEE J. Quantum Electron.* **1984**, *20*, 265−275.

(18) Schmitt-Rink, S.; Chemla, D. S.; Miller, D. A. B. Linear and Nonlinear Optical Properties of Semiconductor Quantum Wells. *Adv. Phys.* **1989**, *38*, 89−188.

(19) Chernikov, A.; Berkelbach, T. C.; Hill, H. M.; Rigosi, A.; Li, Y.; Aslan, O. B.; Reichman, D. R.; Hybertsen, M. S.; Heinz, T. F. Exciton Binding Energy and Nonhydrogenic Rydberg Series in Monolayer WS_2. *Phys. Rev. Lett.* **2014**, *113*, 076802.

(20) Manteiga Vázquez, F.; Yu, Q.; Klepzig, L. F.; Siebbeles, L. D. A.; Crisp, R. W.; Lauth, J. Probing Excitons in Ultrathin PbS Nanoplatelets with Enhanced Near-Infrared Emission. *J. Phys. Chem. Lett.* **2021**, *12*, 680−685.

(21) Semonin, O. E.; Johnson, J. C.; Luther, J. M.; Midgett, A. G.; Nozik, A. J.; Beard, M. C. Absolute Photoluminescence Quantum Yields of IR-26 Dye, PbS, and PbSe Quantum Dots. *J. Phys. Chem. Lett.* **2010**, *1*, 2445−2450.

(22) Caram, J. R.; Bertram, S. N.; Utzat, H.; Hess, W. R.; Carr, J. A.; Bischof, T. S.; Beyler, A. P.; Wilson, M. W. B.; Bawendi, M. G. PbS Nanocrystal Emission is Governed by Multiple Emissive States. *Nano Lett.* **2016**, *16*, 6070−6077.

(23) Shinada, M.; Sugano, S. Interband Optical Transitions in Extremely Anisotropic Semiconductors. I. Bound and Unbound Exciton Absorption. *J. Phys. Soc. Jpn.* **1966**, *21*, 1936−1946.

(24) Yang, X. L.; Guo, S. H.; Chan, F. T.; Wong, K. W.; Ching, W. Y. Analytic Solution of a Two-Dimensional Hydrogen Atom. I. Nonrelativistic Theory. *Phys. Rev. A* **1991**, *43*, 1186−1196.

(25) Kulik, L. V.; Kulakovskii, V. D.; Bayer, M.; Forchel, A.; Gippius, N. A.; Tikhodeev, S. G. Dielectric Enhancement of Excitons in Near-Surface Quantum Wells. *Phys. Rev. B* **1996**, *54*, R2335−R2338.

(26) Keldysh, L. V. Coulomb Interaction in Thin Semiconductor and Semimetal Films. *J. Exp. Theor. Phys.* **1979**, *29*, 658.

(27) Kumagai, M.; Takagahara, T. Excitonic and Nonlinear-Optical Properties of Dielectric Quantum-Well Structures. *Phys. Rev. B* **1989**, *40*, 12359−12381.

(28) Andryushin, E. A. Excitons in Thin Semiconductor Films. *Sov. Phys. Solid State* **1980**, *22*, 1562−1564.

(29) Wetzel, C.; Winkler, R.; Drechsler, M.; Meyer, B. K.; Rössler, U.; Scriba, J.; Kotthaus, J. P.; Härle, V.; Scholz, F. Electron Effective Mass and Nonparabolicity in Ga0.47In0.53As/InP Quantum Wells. *Phys. Rev. B* **1996**, *53*, 1038−1041.

(30) Lauth, J.; Failla, M.; Klein, E.; Klinke, C.; Kinge, S.; Siebbeles, L. D. A. Photoexcitation of PbS Nanosheets Leads to Highly Mobile Charge Carriers and Stable Excitons. *Nanoscale* **2019**, *11*, 21569−21576.

(31) Kane, E. O. Band Structure of Indium Antimonide. *J. Phys. Chem. Solids* **1957**, *1*, 249−261.

(32) Kang, I.; Wise, F. W. Electronic Structure and Optical Properties of PbS and PbSe Quantum Dots. *J. Opt. Soc. Am. B* **1997**, *14*, 1632.

(33) Bohn, B. J.; Tong, Y.; Gramlich, M.; Lai, M. L.; Döblinger, M.; Wang, K.; Hoye, R. L. Z.; Müller-Buschbaum, P.; Stranks, S. D.; Urban, A. S.; et al. Boosting Tunable Blue Luminescence of Halide Perovskite Nanoplatelets through Postsynthetic Surface Trap Repair. *Nano Lett.* **2018**, *18*, 5231−5238.

(34) Gramlich, M.; Lampe, C.; Drewniok, J.; Urban, A. S. How Exciton-Phonon Coupling Impacts Photoluminescence in Halide Perovskite Nanoplatelets. *J. Phys. Chem. Lett.* **2021**, *12*, 11371−11377.

(35) Dalven, R. A Review of the Semiconductor Properties of PbTe, PbSe, PbS and PbO. *Infrared Phys.* **1969**, *9*, 141−184.

(36) Zaslow, B.; Zandler, M. E. Two-Dimensional Analog to the Hydrogen Atom. *Am. J. Phys.* **1967**, *35*, 1118−1119.

(37) Wang, F.; Dukovic, G.; Brus, L. E.; Heinz, T. F. Time-Resolved Fluorescence of Carbon Nanotubes and its Implication for Radiative Lifetimes. *Phys. Rev. Lett.* **2004**, *92*, 177401−4.

(38) Li, Z.; Qin, H.; Guzun, D.; Benamara, M.; Salamo, G.; Peng, X. Uniform Thickness and Colloidal-Stable CdS Quantum Disks with Tunable Thickness: Synthesis and Properties. *Nano Research* **2012**, *5*, 337−351.

(39) Feldmann, J.; Peter, G.; Göbel, E. O.; Dawson, P.; Moore, K.; Foxon, C.; Elliott, R. J. Linewidth Dependence of Radiative Exciton Lifetimes in Quantum Wells. *Phys. Rev. Lett.* **1987**, *59*, 2337−2340.

(40) Moreels, I.; Lambert, K.; Smeets, D.; De Muynck, D.; Nollet, T.; Martins, J. C.; Vanhaecke, F.; Vantomme, A.; Delerue, C.; Allan, G.; et al. Size-Dependent Optical Properties of Colloidal PbS Quantum Dots. *ACS Nano* **2009**, *3*, 3023−3030.

📖 Recommended by ACS